

Molecular dynamics approach on intermolecular interaction between n-icosane and gemini surfactant assisted nanoparticles

Shamala Devi Vijayakumar, Junaidi Zakaria, Norida Ridzuan*

Author's Faculty of Chemical and Process Engineering Technology, Universiti Malaysia Pahang, 26300, Gambang, Pahang, Malaysia

ARTICLE INFO

Article history:

Received 25 July 2021

Received in revised form

1 December 2021

Accepted 1 December 2021

Available online xxx

Keywords:

Gemini surfactant

Nanoparticles

rdf analysis

Intermolecular interaction

Temperature

ABSTRACT

Wax molecules tend to aggregate, and form wax solid at low temperature and result in a wax deposition. Chemical wax inhibitors are introduced to prevent wax deposition. However, the performance of chemical wax inhibitors is temperature dependent. Computational method using Molecular Dynamics (MD) simulation is used in this research to investigate how temperature affects wax inhibition using 2,5,8,11 Tetramethyl 6 dodecyn-5,8 Diol Ethoxylate Gemini surfactant (GS) and nanoparticles silicon dioxide (NP1), tin oxide (NP2), and nickel oxide (NP3). Wax-wax interaction of H58...H61 of n-icosane and wax-solute interaction of hydrogen atom from n-icosane wax and carbonyl oxygen atoms from GS and NPs was investigated via radial distribution function analysis (rdf). The findings revealed that GS/NPs blends have a better chance of wax inhibition than corresponding individuals. Besides that, wax-wax interaction was strongest at 288K, indicating the higher chances of wax formation at low temperature. MD simulation is a promising tool for identifying atoms responsible for the wax formation and inhibition and can be used for chemical wax inhibitor screening for different temperature.

© 2021 Chinese Petroleum Society. Publishing services provided by Elsevier B.V. on behalf of KeAi Communication Co. Ltd. This is an open access article under the CC BY-NC-ND license (<http://creativecommons.org/licenses/by-nc-nd/4.0/>).

1. Introduction

Wax deposition can cause a reduction or suspension in operation by restricting crude oil flowing through the pipeline, generating pressure irregularities, and creating mechanical restrictions. However, in the worst-case scenario, a pipeline or production facility might be shut down. The temperature of the pipeline wall, crude oil flow rate, and residence duration are the factors that influence wax deposition (Junyi and Hasan, 2018). When high-temperature crude oil (70–120 °C) from deep-sea aquifers travels through pipes on the ocean's surface (4 °C), wax solids start to build up on the pipe wall due to heat loss from the crude oil to the ocean (Huang et al., 2011).

Wax deposition often occurs when the temperature of the bulk oil and its cloud point is lower than wax appearance temperature (WAT). If the temperature of the crude oil is above WAT, wax deposition is driven by a low temperature inflow coolant (Kelechukwu et al., 2010; Theyab, 2018). The temperature of the inflow coolant plays an important role in wax build-up. Few studies

investigated the effect of temperature on wax deposition and wax inhibition by using chemical wax inhibitors. Past research showed that temperature had impacted the performance of wax inhibitors and the deposition of wax (Anisuzzaman et al., 2017; Ridzuan and Al-Mahfadi, 2017).

The temperature's impact on reducing the viscosity of Malaysian crude oil has been widely investigated. Subramanie et al. (2020) studied the performance of wax inhibitors poly ethylene-co-vinyl acetate (EVA) and poly maleic anhydride-alt-1-octadecene (MA) and sodium cloisite Na + as viscosity reducers at different temperature. The study yielded results showing that EVA, MA, and nanoparticles significantly lowered crude oil viscosity at temperatures below the WAT. Still, the viscosity of crude oil had a minimal effect as the temperature reached the WAT.

According to VijayaKumar et al. (2021a,b), crude oil viscosity is reduced using a Gemini surfactant with and without nanoparticles, silicon dioxide, tin oxide, and nickel (III) oxide. The wax inhibitors reduced the viscosity of the crude oil at temperatures approaching the pouring point. At 10–15 °C, it is possible to see the effect of viscosity drop. The flow improvers had no impact on oil viscosity closer to the WAT. Also, VijayaKumar et al. (2021) added that the addition of nanoparticle-Gemini blend shows a significant result at low temperature, showing the best reduction of crude oil viscosity.

* Corresponding author.

E-mail addresses: shamalad125@gmail.com (S.D. Vijayakumar), junaidibz@ump.edu.my (J. Zakaria), norida@ump.edu.my (N. Ridzuan).

<https://doi.org/10.1016/j.ptlrs.2021.12.001>

2096-2495/© 2021 Chinese Petroleum Society. Publishing services provided by Elsevier B.V. on behalf of KeAi Communication Co. Ltd. This is an open access article under the CC BY-NC-ND license (<http://creativecommons.org/licenses/by-nc-nd/4.0/>).

Higher temperature showed less effect of viscosity reduction. There was only a limited amount of solid wax at those temperatures (Pedersen and Rønningsen, 2003).

To improve the visual knowledge of the wax inhibitor efficiency toward wax deposition in crude oil, MD is performed. Previous research has not considered MD studies to gain a better understanding of molecular-level interactions. The goal of this paper is to use MD simulation to investigate the interaction between wax molecules, Gemini surfactant 2,5,8,11 Tetramethyl 6 dodecyn-5,8 Diol Ethoxylate (GS) and nanoparticles silicon dioxide (NP1), tin oxide (NP2), and nickel oxide (NP3) at various temperatures (15–35 °C).

2. Methodology

2.1. Molecular dynamics simulation

The MD simulation was run on an HP Z400 computer with Accelrys Material Studio 8. It was done with the Forcite module's dynamic tasks for structure optimization and minimization calculation. The mixture density was used to generate a cubical simulation box with a periodic border for the initial condition of wax and inhibitor. A 200–300 ps run in the NVE ensemble was used for equilibration, followed by a 1000 ps run in the NVT ensemble with a 1 fs stepsize. All simulations were conducted at the desired temperature (288K, 298K, 308K) and pressure. The COMPASS force field detailed the molecules' intermolecular interactions (Ridzuan et al., 2014). The Nose thermostat is used for temperature management in NVT ensembles with a constant number of atoms, volume, and temperature, with a Q ratio of 1.0.

To characterize non-bonded energies in periodic systems, the motion equations were combined using the Verlet algorithm with an atom-based summation approach. The rdf was used to analyze the trajectory file generated by the dynamic simulations. The rdf is a structural feature that measures the likelihood of discovering nearby molecules at a certain r distance from the reference

molecule. The following equation, Eq (1) can be used to define the probability $g(r)$.

$$g_{xy}(r) = \frac{\langle N_y(r, r + dr) \rangle}{\rho_y 4\pi r^2 dr} \quad (1)$$

r = spherical radius

ρ_y = density of an atom

N_y = number of y atom

Following the rdf analysis, a graph of $g(r)$ vs. reduced distance, r was generated and analyzed to observe how wax and inhibitor molecules interacted. Fig. 1 depicts the molecular structure of wax (n-icosane), Gemini surfactant, and nanoparticles. Table 1 shows the details of pure, binary and tertiary systems.

2.2. Paraffin inhibition efficiency (PIE)

The study involved using cold finger apparatus to determine the amount of wax and the performance of wax inhibitors. The experimental setup was similar to cold finger analysis by (Ridzuan et al., 2016). The water bath was kept up at 50 °C. The screening of wax inhibitor experimental duration was fixed at 2 h, cold finger temperature at 5 °C, and the rotational speed of the impeller of 300 rpm. The wax deposit from the cold finger was weighed to determine the PIE, as shown in Eq (2) (Lim et al., 2018).

$$PIE (\%) = \frac{W_f - W_t}{W_f} \times 100 \quad (2)$$

where w_f is the reference weight of wax deposition without chemical treatment (g) and w_t is the weight of paraffin deposition with chemical treatment (g).

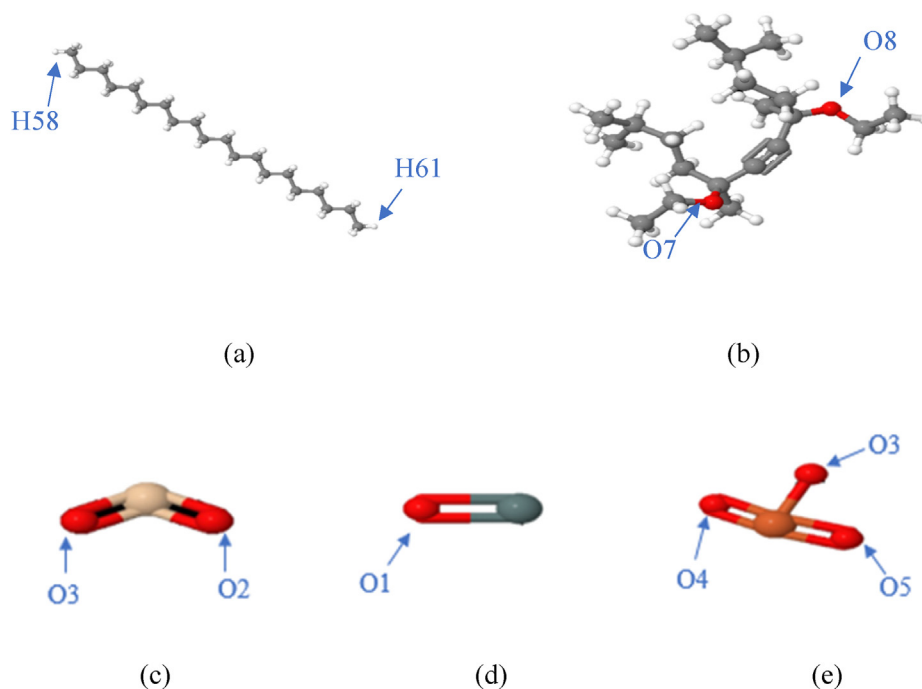


Fig. 1. Molecular structure of nanoparticles and their active atoms; (a) Wax, (b) Wax inhibitor, (c) silicon dioxide (NP1), (d) tin (II) oxide (NP2), (e) nickel (III) oxide (NP3).

Table 1
Simulation and input parameters to represent the wax inhibition.

Molecules	No. of molecules	Density(g/cm ³)	Box size, A × B × C
Pure system:			36.24 × 36.24 × 36.24
Wax	80	0.7886	
Binary system:			
Wax: GS	80:20	0.8048	38.68 × 38.68 × 38.68
Wax: NP1	80:10	0.8032	36.33 × 36.33 × 36.33
Wax: NP2	80:10	0.8349	36.25 × 36.25 × 36.25
Wax: NP3	80:10	0.8354	36.06 × 36.06 × 36.06
Tertiary system:			
Wax: GS: NP1	80:20:10	0.8343	38.48 × 38.48 × 38.48
Wax: GS: NP2	80:20:10	0.8603	38.42 × 38.42 × 38.42
Wax: GS: NP3	80:20:10	0.8607	37.86 × 37.86 × 37.86

3. Results and discussion

3.1. The effect of temperature on wax-wax interaction

Temperature is one of the factors influencing wax deposition. Therefore, the injection of wax inhibitor needs to be considered. The performance of wax inhibitors is dependent on the temperature (Ragunathan et al., 2020). Some chemical inhibitors are highly efficient at low temperature, while some are efficient at high temperature. Thus, the effect of temperature was investigated on the intermolecular interaction between wax-solute at 288K (below WAT), 298K (room temperature), and 308K (above WAT) for both binary and tertiary systems. The WAT is 28 °C. Fig. 2, Fig. 3 and Fig. 4 represents the rdf pattern on wax-wax interaction in the pure wax system and Gemini surfactant and nanoparticles in binary and tertiary systems, respectively. Table 2 summarizes the rdf shift of pure, binary, and tertiary systems.

As shown in Table 2 and Fig. 2, for the pure wax system, the rdf value is shifted from 2.75 Å to 3.25 Å as the temperature increases, implying to lesser van der Waals (vdW) interaction between H58···H61 molecules. Wax-wax interaction implies wax aggregation. As the stage of wax precipitation, nucleation occurs when the temperature of the crude oil decreases to the WAT. The wax molecules cluster together, giving the surface a cloudy appearance, hence the term “cloud point,” which refers to the WAT value. The paraffin wax molecules gradually bond and dissociate until they reach the desired size cluster, at which stage they become stable.

Above WAT, lesser wax will be formed.

Comparing 288K (below WAT) and 308K (above WAT), the presence of Gemini surfactant and nanoparticles for the binary and tertiary system have increased the rdf value of H58···H61 at a temperature above WAT. This means temperature plays an important role in wax agglomeration, where at low temperatures, wax molecules tend to aggregate even in the presence of GS and NPs. The performance of chemical wax inhibitors is temperature-dependent (Ragunathan et al., 2020). Referring to Table 2, GS showed the highest wax solubility at 308K with rdf value of 4.25 Å. Meanwhile, all three NPs with and without GS showed better wax solubility at 298K with a high rdf value as seen in Table 2. Following the rdf shift of H58···H61, which reflects wax solubility, the possible order of wax inhibition efficiency of GS and NPs is as listed in Table 3.

Overall, GS and NPs have the strongest interaction at a temperature below WAT. Above WAT, the wax solids are usually in a lower amount compared to below WAT. Thus, the possibility of GS and NPs interacting with wax molecules is lower. This explains the reason behind the low $g(r)$ value for the overall rdf pattern at 308K. GS and NPs can adsorb onto the surface of the wax, preventing them from aggregating and forming wax solids. In GS/NPs blend, the number of carbonyl oxygen atom is higher than separately in GS and NPs systems. Thus, the possibility of hydrogen atom encountering oxygen atoms is higher in GS/NPs blend tertiary system.

The temperature where the first wax crystals are noticed during the oil cooling is called the WAT (Mendes, 2015). At temperature above WAT, wax molecules are barely to form. The high molecular weight paraffin is usually dissolved in the liquid matrix that makes up the oil at the temperature of the petroleum reservoir. However, as the temperature drops, their solubility declines (Singh et al., 2000).

3.2. Intermolecular interaction between wax and solute

The intermolecular interaction was investigated between the hydrogen atom of n-icosane towards the carbonyl oxygen atoms of GS, NP1, NP2, and NP3 in the binary and tertiary system at 288 K, 298 K, and 308 K. Fig. 5 to Fig. 8 represent wax-solute interaction of the binary and tertiary system of GS and NPs. Table 4 and Table 5 summarizes the rdf shift for GS and NPs, respectively.

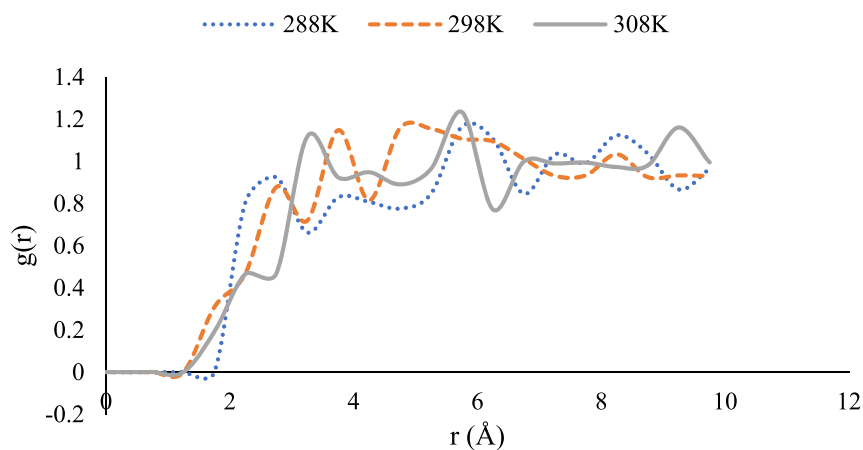


Fig. 2. The rdf pattern of H58···H61 interaction in the pure wax system at different temperature.

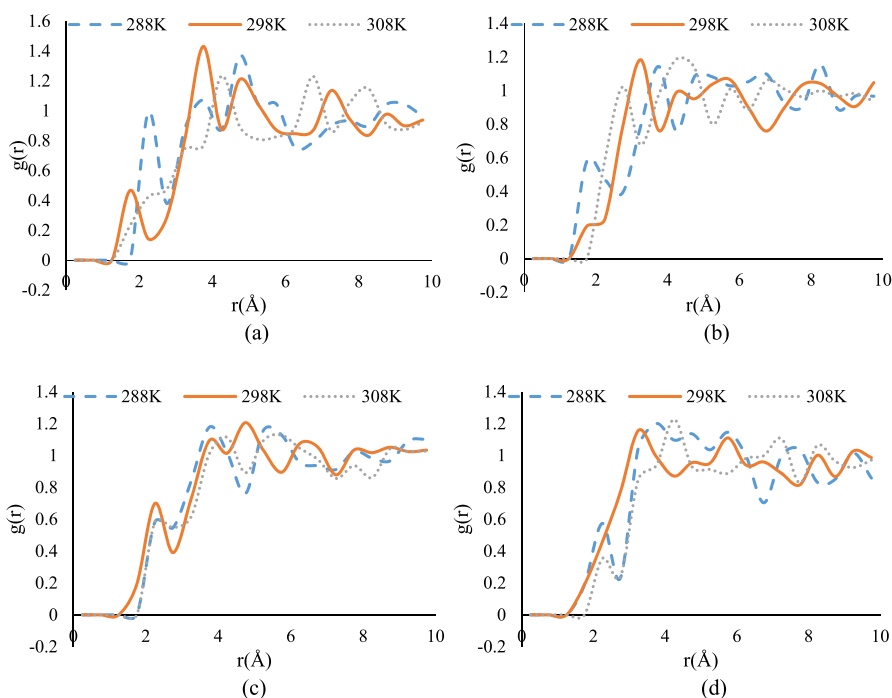


Fig. 3. The rdf pattern for H58...H61 of n-icosane at different temperature in (a) GS, (b) NP1 (c) NP2, and (d) NP3.

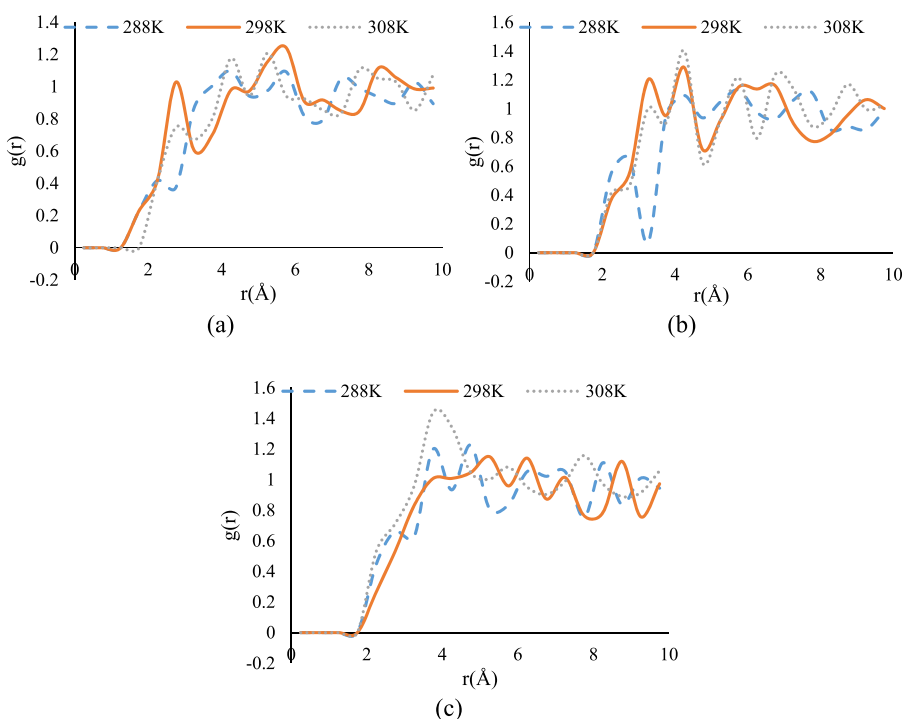


Fig. 4. The rdf pattern of H58...H61 of n-icosane in: (a) GS/NP1, (b) GS/NP2, and (c) GS/NP3.

Fig. 5 shows the rdf pattern for wax-solute interaction of H58 from n-icosane and O7 from GS. Referring to Table 4, the first neighbouring atom of the intermolecular interaction of H58...O7 in GS is at 2.75 Å for both 288K and 308K. As the temperature increases, the rdf value is shifted to 4.25 Å for 298 K. This implies that

the interaction of wax and GS molecules is stronger at 288 K and 308K. In the presence of nanoparticles, the interaction of GS molecules with wax was improved at 288 K except for GS/NP1, where the distance between interacting atoms is higher. At 298K, the interaction of H58...O7 was stronger in all tertiary systems, as

Table 2
rdf value for H58...H61 interaction at different temperatures.

Component	System	rdf, Å		
		288K	298K	308K
Wax-wax	Pure	2.75	2.75	3.25
Wax-GS	Binary	2.25	1.75	4.25
Wax-NP1		1.75	3.25	2.75
Wax-NP2		2.25	2.25	2.25
Wax-NP3	Tertiary	2.25	3.25	2.25
Wax-GS/NP1		2.25	2.75	2.75
Wax-GS/NP2		2.75	3.25	3.25
Wax-GS/NP3		3.75	5.25	3.75

Table 3
Possible order of wax inhibition efficiency at different temperature.

Temperature, K	Possible order of wax inhibition efficiency
288	GS/NP3 > GS/NP2 > GS > NP2 > NP3 > GS/NP1 > NP1
298	GS/NP3 > GS/NP2 > NP1 > NP3 > GS/NP1 > NP2 > GS
308	GS > GS/NP3 > GS/NP2 > GS/NP1 > NP1 > NP2 > NP3

indicated by lower rdf values. As the temperature increased to 308 K, the presence of nanoparticles NP 1 and NP 2, the rdf value of H58...O7 was similar to GS's binary system, implying that nanoparticles did not affect in enhancing GS efficiency. However, the rdf value was lower in GS/NP3 system.

Overall, the rdf shift showed better interaction in tertiary systems compared to a binary system. The addition of nanoparticles can enhance the surface activity of surfactants (Lim et al., 2018). Thus, in the presence of nanoparticles, GS molecules can form stronger interactions with wax molecules. This supports the results from cold finger analysis which showed higher PIE% when GS/NPs blend was used compared to GS alone.

Table 4
rdf value for wax-GS interaction with and without the presence of nanoparticles.

Interacting atoms	rdf, Å			
	H58...O7			
Temperature	GS	GS/NP1	GS/NP2	GS/NP3
288 K	2.75	3.25	2.25	2.25
298 K	4.25	2.25	3.25	2.25
308 K	2.75	2.75	2.75	2.25

Table 5
rdf value for wax-nanoparticles interaction with and without the presence of GS.

Interacting atoms	rdf, Å					
	H58...O2		H58...O1		H58...O4	
Temperature	NP1	GS/NP1	NP2	GS/NP2	NP3	GS/NP3
288 K	2.75	3.25	2.75	2.25	3.25	2.25
298 K	2.75	2.25	3.75	3.25	3.25	2.25
308 K	1.75	2.75	2.75	2.75	2.25	2.25

Fig. 6 shows the rdf pattern for H58...O2 in NP1 and GS/NP1 systems. In the binary system of NP1, the first neighbor atom of intermolecular interaction between H58...O2 is at 2.75 Å for 288K, and 298 K. Lowest rdf value was observed at 1.75 Å at 308K. The peak reflects a strong intermolecular interaction that controls the solubility of wax by the presence of NP1. In GS/NP1 system, the rdf value was observed to be increasing for 288 K and 308 K, implying weaker interaction. Whereas, for 298K, the rdf value shifted to 2.25 Å, indicating stronger interaction of wax-solute.

Referring to Fig. 7, the rdf value of H58...O1 is 2.25 Å for 288 K and 308K. A weaker interaction was observed at 298K, with a higher rdf value. H58...O1 interaction reflects a weaker intermolecular interaction to increase the wax solubility and prevent the

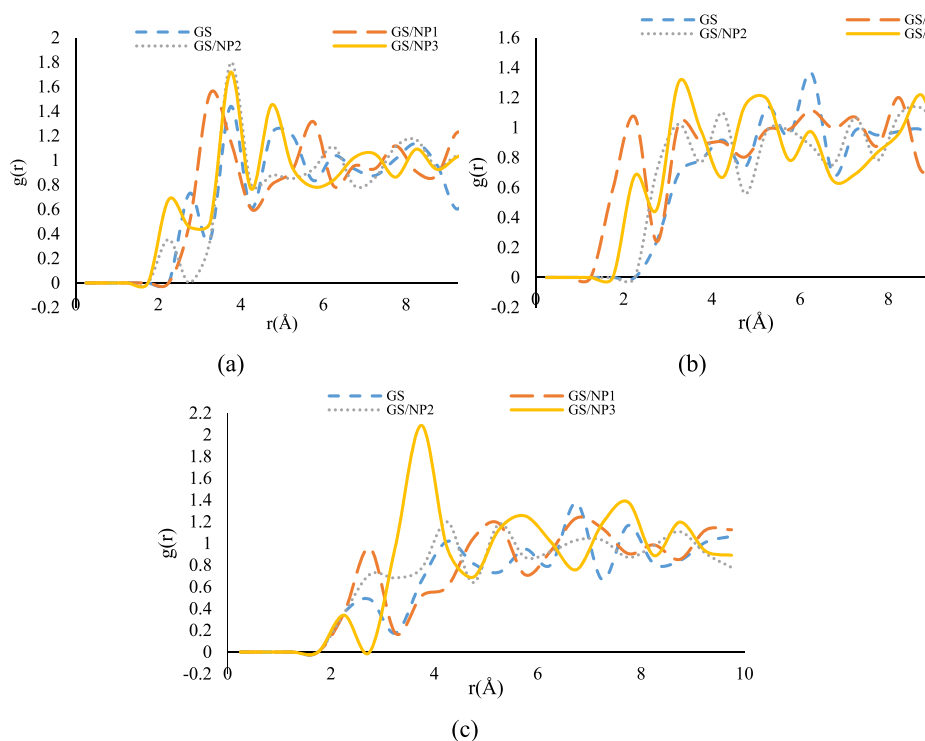


Fig. 5. Wax-solute interaction in the presence of GS and GS/NP blends at; (a) 288K, (b) 298K, and (c) 308K.

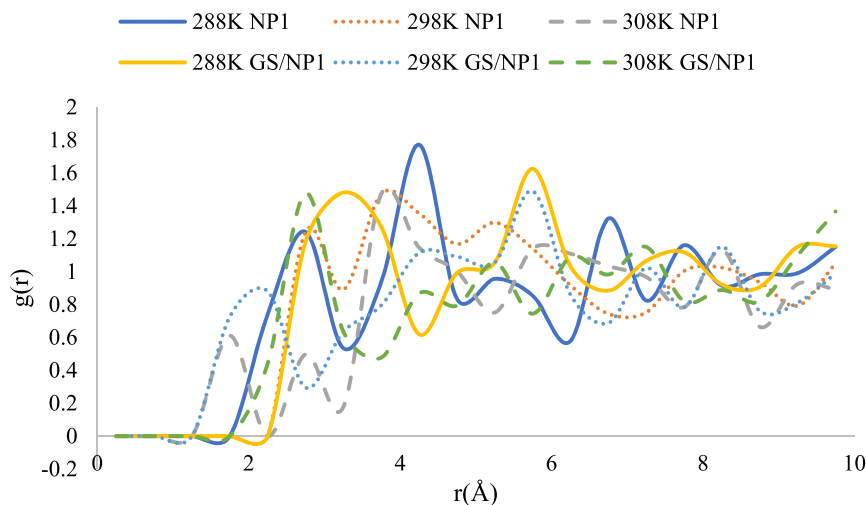


Fig. 6. The rdf pattern for wax-solute of n-Icosane in NP1 and GS/NP1 system.

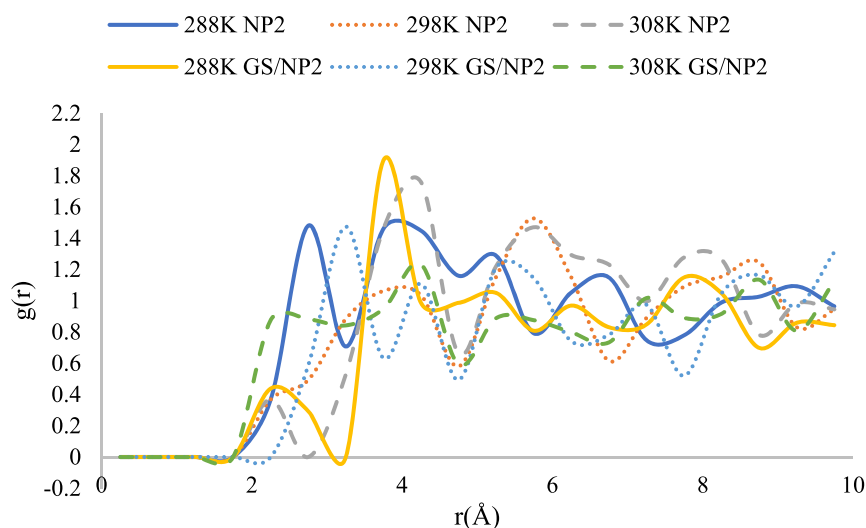


Fig. 7. The rdf pattern for wax-solute of n-Icosane in NP2 and GS/NP2 system.

solid wax formation at 298K. In the presence of GS/NP2, rdf shifts at 288K and 298K indicated stronger interaction compared to the NP2 system, while for 308K, the rdf value was similar to the NP2 system. Fig. 8 shows the rdf pattern for n-icosane and NP3 molecules in NP3 and GS/NP3 systems. In the binary system of NP3, the first neighbor atom of intermolecular interaction between H58...O4 is at 3.25 Å for 288K and 298K and 2.25 Å for 308K. The peaks reflect a strong intermolecular interaction at 308K, which would control the solubility of n-icosane by the presence of NP3. GS/NP3 showed rdf shift to 2.25 Å for all temperatures, indicating stronger intermolecular interaction than the NP3 system.

The notable shifts in rdf value imply that the interaction of wax particles with NPs is stronger in GS/NPs blend systems than their corresponding individual system with weaker intermolecular interaction. This can be due to the O carbonyl group in both GS and NPs, capable of establishing a larger quantity of hydrogen bonds (Ridzuan et al., 2014). When nanoparticles are coated with a

surfactant, the surfactant will act as a stabilizing agent to limit the reaggregation and agglomeration of nanoparticles. Therefore, it reduces the size of the wax (Paramashivaiah and Rajashekhar, 2016). The results wax-solute interaction supports the results from cold finger analysis, where the PIE was higher in GS, and NPs blends compared to their corresponding individuals as presented in Table 6.

The blends of GS and nanoparticles performed better than when they were used separately. Crude oil with a GS/NPs blend has a higher PIE value than the corresponding individuals. This would support the hypothesis that the GS/NP3 blend is responsible for the highest $g(r)$ value and peak. This could be due to the presence of GS, which alters nanoparticle surfaces to improve wax molecule surface adsorption. Wax molecules will be less likely to clump together. Therefore, the probability of the vdW interaction influencing solubility in the GS/NPs blend is higher than in secondary systems, according to this research.

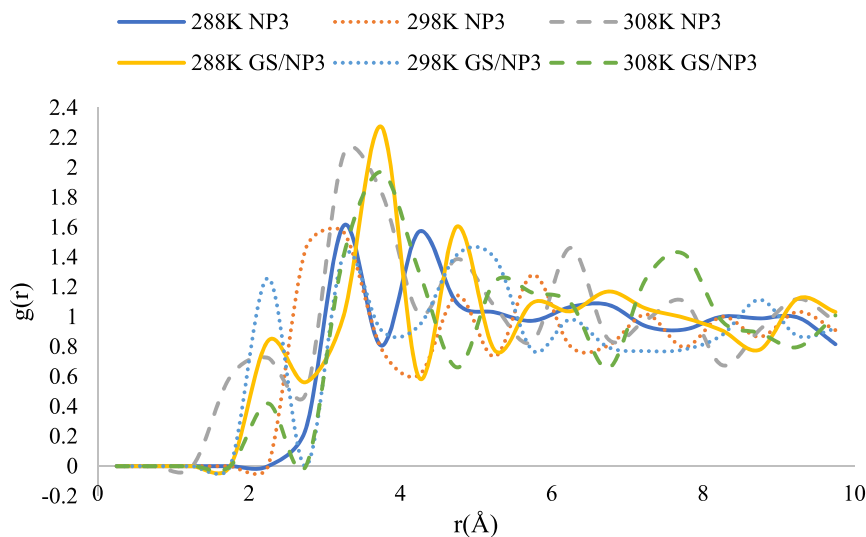


Fig. 8. The rdf pattern for wax-solute of n-icosane in NP3 and GS/NP3 system.

Table 6
Paraffin inhibition efficiency of GS and NPs.

Type of inhibitor	PIE%
GS	46.5
NP1	45.9
NP2	47.2
NP3	47.7
GS/NP1	52.0
GS/NP2	59.0
GS/NP3	61.6

4. Conclusion

The molecular dynamics simulation results showed that the intermolecular interaction between wax molecules and GS and NPs varies at different temperatures. H58···H61 of n-icosane for wax-wax interaction was observed to be strongest at 288K in both binary and tertiary systems. This is due to the presence of a high amount of wax solids below WAT. At high temperature, the wax solids are dissolved. Thus, the possibility of wax-wax interaction is minimal. For wax-solute interaction, the hydrogen atoms from n-icosane wax formed strong vdW interaction with carbonyl oxygen atoms from GS and NPs at the temperature of 298K. The tertiary system of GS/NPs blends showed a higher rdf value for wax-wax interaction compared to the binary system. This is due to the higher number of carbonyl oxygen atoms more likely to interact with a wax molecule, thus preventing them from aggregating. Also, the study concluded that the interaction of wax-solute was stronger in GS/NPs blends than their individuals, which is supported by cold finger analysis results. Molecular dynamics simulation also provides insights on which atom is responsible for wax inhibition. The software is beneficial for screening purposes that can predict a possible performance.

Declaration of competing interest

The authors declare that they have no conflict of interest.

Acknowledgment

The authors gratefully acknowledge the financial support provided by Universiti Malaysia Pahang under Internal Research grant

RDU200302. The authors also extend their appreciation to Petronas Penapisan Terengganu, Malaysia for supplying crude oil sample throughout the study.

References

- Anisuzzaman, S.M., Abang, S., Bono, A., Krishnaiah, D., Karali, R., Safuan, M.K., 2017. Wax inhibitor based on ethylene vinyl acetate with methyl methacrylate and diethanolamine for crude oil pipeline. *IOP Conf. Ser. Mater. Sci. Eng.* 206.
- Huang, Z., Lu, Y., Hoffmann, R., Amundsen, L., Fogler, H.S., 2011. The effect of operating temperatures on wax deposition. *Energy Fuels* 25, 5180–5188.
- Junyi, K., Hasan, N., 2018. Review of the factors that influence the condition of wax deposition in subsea pipelines. *Int. J. Eng. Mater. Manuf.* 3, 1–8.
- Kelechukwu, E.M., Al Salim, H.S.S., Yassin, A.A.M., 2010. Influencing factors governing paraffin wax deposition during crude production. *Int. J. Phys. Sci.* 5, 2351–2362.
- Lim, Z.H., Al Salim, H.S., Ridzuan, N., Nguete, R., Sasaki, K., 2018. Effect of surfactants and their blend with silica nanoparticles on wax deposition in a Malaysian crude oil. *Petrol. Sci.* 15, 577–590.
- Mendes, R., 2015. Rheological behavior and modeling of waxy crude oils in transient flows. *J. Rheol.* 174.
- Paramashivaiah, B.M., Rajashekhar, C.R., 2016. Studies on effect of various surfactants on stable dispersion of graphene nano particles in simarouba biodiesel. *IOP Conf. Ser. Mater. Sci. Eng.* 149.
- Pedersen, K.S., Rønningsen, H.P., 2003. Influence of wax inhibitors on wax appearance temperature, pour point, and viscosity of waxy crude oils. *Energy Fuels* 17, 321–328.
- Ragunathan, T., Husin, H., Wood, C.D., 2020. Wax formation mechanisms, wax chemical inhibitors and factors affecting chemical inhibition. *Appl. Sci.* 10, 1–18.
- Ridzuan, N., Adam, F., Yaacob, Z., 2016. Screening of factor influencing wax deposition using full factorial experimental design. *Petrol. Sci. Technol.* 34, 84–90.
- Ridzuan, N., Adam, F., Yaacob, Z., 2014. Molecular recognition of wax inhibitor through Pour Point Depressant type inhibitor. *Soc. Pet. Eng. - Int. Pet. Technol. Conf.* 2014, IPTC 1649–1657.
- Ridzuan, N., Al-Mahfadi, M., 2017. Evaluation on the effects of wax inhibitor and optimization of operating parameters for wax deposition in Malaysian crude oil. *Petrol. Sci. Technol.* 35, 1945–1950.
- Singh, P., Venkatesan, R., Fogler, H.S., Nagarajan, N., 2000. Formation and aging of incipient thin film wax-oil gels. *AIChE J.* 46, 1059–1074.
- Subramanie, P.A.P., Padhi, A., Ridzuan, N., Adam, F., 2020. Experimental study on the effect of wax inhibitor and nanoparticles on rheology of Malaysian crude oil. *J. King Saud Univ. - Eng. Sci.* 32, 479–483.
- Theyab, M.A., 2018. Wax deposition process: mechanisms, affecting factors and mitigation methods. *J. Sci.* 2.
- VijayaKumar, S.D., Zakaria, J., Ridzuan, N., 2021a. The role of Gemini surfactant and SiO₂/SnO/Ni₂O₃ nanoparticles as flow improver of Malaysian crude oil. *J. King Saud Univ. - Eng. Sci.*
- VijayaKumar, S.D., Zakaria, J., Ridzuan, N., 2021b. The role of nanoparticle-gemini surfactant to improve the flowability of the Malaysian crude. *Oil. Lect. Notes Mech. Eng.* 271–281.